Research paper

Development of a data-driven forecasting tool for hydraulically fractured, horizontal wells in tight-gas sands

B. Kulga[a],[*], E. Artun[b], T. Ertekin[a]

[a] Pennsylvania State University, John and Willie Leone Family Department of Energy and Mineral Engineering, University Park, PA 16802, USA
[b] Middle East Technical University, Northern Cyprus Campus, Petroleum and Natural Gas Engineering Program, Mersin 10 99738, Turkey

ARTICLE INFO

ABSTRACT

Tight-gas sand reservoirs are considered to be one of the major unconventional resources. Due to the strong heterogeneity and very low permeability of the formation, and the complexity of well trajectories with multiple hydraulic fractures; there are challenges associated with performance forecasting and optimum exploitation of these resources using conventional modeling approaches. In this study, it is aimed to develop a data-driven forecasting tool for tight-gas sands, which is based on artificial neural networks that can complement the physics-driven modeling approach, namely numerical-simulation models. The tool is designed to predict the horizontal-well performance as a proxy to the numerical model, once the initial conditions, operational parameters, reservoir/hydraulic-fracture characteristics are provided. The data-driven model, that the forecasting tool is based on, is validated with blind cases by estimating the cumulative gas production after 10 years with an average error of 3.2%. A graphical-user-interface application is developed that allows the practicing engineer to use the developed tool in a practical manner by visualizing estimated performance for a given reservoir within a fraction of a second. Practicality of the tool is demonstrated with a case study for the Williams Fork Formation by assessing the performance of various well designs and by incorporating known uncertainties through Monte Carlo simulation. P10, P50 and P90 estimates of the horizontal-well performance are quickly obtained within acceptable accuracy levels.

1. Introduction

Increasing demand for fossil fuels and the decline in their production have been promoting the production from unconventional resources during the last few decades. Together with the enhancements in drilling and production technologies, it has recently become technically and practically feasible to produce hydrocarbons stored in some of these unconventional resources such as shale/tight reservoirs. This has been offering a huge potential for the increasing production of fossil fuels on a global scale. Among unconventional resources, tight-gas sand reservoirs are considered to be a major resource with a most-likely estimate of the original-gas-in-place of 71,981 TCF worldwide (Dong et al., 2012). The standard industry definition of tight-gas is framed as the producible natural gas from reservoirs that have permeability values less than 0.1 md, which usually occurs in sand-stone formations, shale formations, and coal seams (Law and Curtis, 2002). Some reservoirs may even have in-situ permeability values as low as 0.000001 md. Even though the definition of *tight* is based on the permeability, these reservoirs also often have porosity values less than

10% (Smith et al., 2009).

Although tight-gas reservoirs have been known for many decades, production from these resources had not been commercially feasible and technologically available until late 1970s (Law and Curtis, 2002). Due to the strong heterogeneity of tight-gas formations, pores are connected by very narrow capillaries and this results in very low permeability in millidarcy to nanodarcy ranges, as demonstrated by two sandstone samples from Williams Fork Formation of Colorado Basin (Metz et al., 2009). Due to unique geologic characteristics of tight-gas sands, conventional, vertical-well based production technologies become insufficient to recover these resources, making it necessary to drill horizontal wells with multiple hydraulic fractures along the wellbore. This results in a characteristic of tight-gas reservoirs as "a reservoir that cannot be produced at economic flow rates nor recover economic volumes of natural gas unless the well is stimulated by a large hydraulic fracture treatment or produced by use of a horizontal wellbore or multilateral wellbores" (Holditch, 2006). Horizontal wellbores help operators to place geometrically more transverse and discrete hydraulic fractures, and thus, realizing a

significant opportunity to increase the gas production (Baihly et al., 2009). Hydraulic fractures, therefore, allow to increase the surface area in contact with the production zone, resulting in improved well productivity. They also decrease the well's drawdown and create highly conductive paths for production (Medeiros et al., 2008).

Aforementioned features of tight-gas reservoirs create challenges to utilize proper reservoir management practices and efficient decision-making workflows, unless proper knowledge management, data assimilation and data analysis practices are in place. These practices can be realized with models that can be updated quickly when new data are available, while representing the actual system accurately (Artun, 2016). Only then, these models can be used for decision-making purposes with confidence.

While numerical reservoir simulation, a physics-driven modeling approach, is recognized as the standard decision-making approach in the petroleum industry, today's fast-paced business environment often requires faster decision-making workflows. It is aimed to develop workflows that can use the collected data to update existing models and provide improved forecasts within a reasonable amount of time. As an alternative approach to physics-driven modeling, data-driven models mimic the functional relationship between process variables through a training process using available data (observations). The main difference between a data-driven model and a physics-driven model is the existence of presumed functional relationships to define physical phenomena in physics-driven models. Data-driven models do not presume any functional relationship, and the physical phenomena are captured via the signatures (patterns) that exist in the data observed. Data-driven modeling approach is a promising way of achieving the aforementioned objectives regarding the model characteristics of being fast, accurate and representative. The primary benefits of this approach become more evident in one of the following conditions:

1. When there is not an existing, reliable physics-driven model (such as a high-fidelity numerical reservoir model),
2. When a comprehensive study using the physics-driven model takes a longer time than desired, or requires significant resources in terms of finances, manpower and computational power.

In reservoir engineering, at least one of these conditions typically exist, since the most critical data can be collected only from well locations, and construction/validation of numerical models typically require significant resources that may not be easy to afford.

Considering the common characteristics of tight-gas sand reservoirs, these systems may be considered as ideal candidates for successful utilization of the data-driven modeling approach. Model-building process and quick evaluation of reservoir performance are resource-demanding due to existence of horizontal wells with multiple hydraulic fractures (Abacioglu et al., 2009). In this study, it is aimed to develop a data-driven forecasting tool that can be used to address these issues by complementing the physics-driven modeling approach, namely numerical simulation models. This simulation-based proxy tool can be integrated into reservoir management protocols with confidence to quickly estimate the reservoir performance. While the tool developed has similar limitations with those of a numerical model, the efficiency in the computational time allows the practicing engineer to achieve the modeling objectives and to reduce the uncertainty ranges in a rapid way. The scope of this study includes development of a data-driven model specifically for horizontal wells with multiple hydraulic fractures in tight-gas sands, structure of which is also presented in Fig. 1. It is aimed to use this model as a forecasting tool that can predict the horizontal well performance, once the initial conditions, operational parameters, reservoir/hydraulic-fracture characteristics are provided, as a proxy to the numerical reservoir simulator.
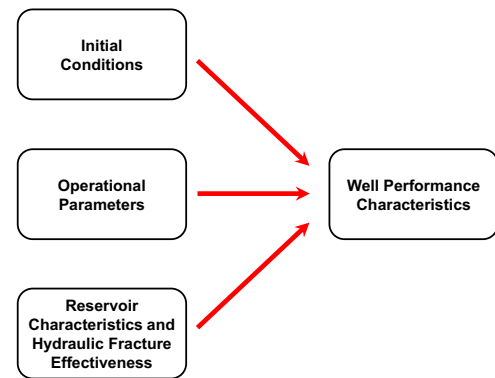

Fig. 1. Structure of the data-driven model developed for forecasting the performance of horizontal wells in tight-gas sands.

2. Methodology

2.1. Data-driven modeling

Data-driven modeling mainly encompasses computational intelligence and machine learning methods that can be used to build models for complementing or replacing physics-based models (Solomatine et al., 2008). Before starting to build a data-driven model, it is critically important to clearly identify the primary objectives of the model so that its scope is also defined. Process variables to be considered for the model can be defined depending on the objectives, including the parameters needed for decision-making purposes. Together with the objectives, availability and quality of the data must also be considered not to overestimate the capabilities of the model developed. Subject-matter experts would identify any inconsistencies and additional data requirements. After identifying the objectives and data inventory, the model-development process can be initiated. Two steps of developing a data-driven model, as applied to reservoir engineering, can be summarized as the following (Mohaghegh, 2011):

1. Development of a spatial-temporal database: This step includes collecting a large set of spatial-temporal instances of the reservoir, represented by collected data (production volumes, pressures, well logs, etc.). The data collected would preferably be real data. However, if good-quality real data do not exist, synthetic data from models can be used (soft data; such as data from a numerical or analytical model).
2. Training the model: This step includes determining the method to be used to construct the model, choosing the appropriate training algorithm and feeding the algorithm with the spatio-temporal database, such that the model has been presented patterns from the reservoir. After properly validating the predictive model (with realistic blind cases that are not introduced to the model during training), the model can be used as a prediction tool.

In this study, a numerical reservoir simulator is used to generate the spatio-temporal instances of the reservoir within pre-determined ranges of certain input parameters. A black-oil reservoir model that represents the drainage area of a horizontal well with multiple hydraulic fractures in a tight-gas sand reservoir is constructed using a commercial reservoir simulator (CMG, 2015), characteristics of which are given in Section 2.2. Since single-phase gas flow is simulated, black-oil formulation can accurately represent the fluid flow as also demonstrated in other simulation studies for tight-gas sands (Iwere et al., 2006). Artificial neural networks are selected as the training method, which have been successfully utilized in many science and engineering problems to extract complex and non-linear relationships between process variables. In the petroleum industry, several areas of
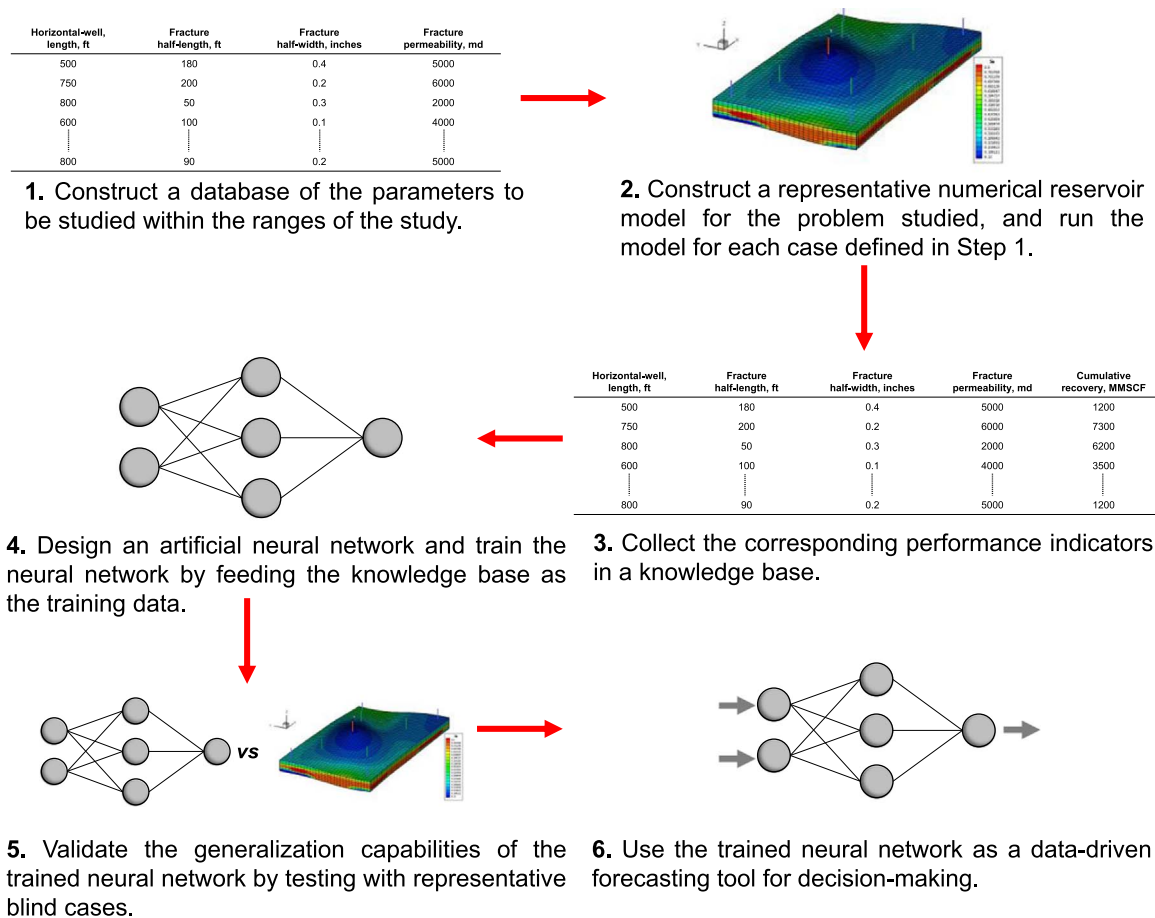
Horizontal-well, length, ft	Fracture half-length, ft	Fracture half-width, inches	Fracture permeability, md
500	180	0.4	5000
750	200	0.2	6000
800	50	0.3	2000
600	100	0.1	4000
800	90	0.2	5000

1. Construct a database of the parameters to be studied within the ranges of the study.

2. Construct a representative numerical reservoir model for the problem studied, and run the model for each case defined in Step 1.

4. Design an artificial neural network and train the neural network by feeding the knowledge base as the training data.

Horizontal-well, length, ft	Fracture half-length, ft	Fracture half-width, inches	Fracture permeability, md	Cumulative recovery, MMSCF
500	180	0.4	5000	1200
750	200	0.2	6000	7300
800	50	0.3	2000	6200
600	100	0.1	4000	3500
800	90	0.2	5000	1200

3. Collect the corresponding performance indicators in a knowledge base.

5. Validate the generalization capabilities of the trained neural network by testing with representative blind cases.

6. Use the trained neural network as a data-driven forecasting tool for decision-making.

Fig. 2. The workflow followed to develop a data-driven forecasting tool using artificial neural networks, adapted from Artun et al., 2012.

application included reservoir characterization (Artun and Mohaghegh, 2011; Raeesi et al., 2012; Alizadeh et al., 2012), well-placement/ trajectory optimization (Centilmen et al., 1999; Doraisamy et al., 2000; Johnson and Rogers, 2001; Gokcesu et al., 2005; Mohaghegh et al., 2014), screening and optimization of secondary/enhanced oil recovery processes (Ayala and Ertekin, 2005; Patel et al., 2005; Demiryurek et al., 2008; Artun et al., 2010, 2011, 2012; Parada and Ertekin, 2012; Amirian et al., 2013), history matching (Cullick et al., 2006; Silva et al., 2007), reservoir modeling, monitoring and management (Zangl et al., 2006; Mohaghegh, 2011; Mohaghegh et al., 2014), and performance forecasting of unconventional gas resources (Kalantari-Dhaghi et al., 2015; Esmaili and Mohaghegh, 2016).

The workflow followed to construct a data-driven model by incorporating a numerical reservoir model and artificial neural networks can be summarized in the following step-by-step procedure, as also shown in Fig. 2:

1. After defining the process parameters that are going to be varied, and setting the ranges and statistical distributions of these parameters, a database is constructed with a large number of different cases within the ranges studied. At this stage, performance indicators that are going to be used for decision-making should also be identified.
2. A numerical reservoir model that represents the problem under consideration is constructed in a way that process parameters can be input to the model and performance indicators can be collected as outputs. All cases generated in Step 1 are run using the numerical reservoir model.
3. For each case, corresponding performance indicators are collected in a knowledge base.
4. The knowledge base is fed into the training model, which is the

artificial neural network constructed for the problem under consideration.
5. The model is validated with representative blind cases.
6. The model is used as a data-driven forecasting tool for decision-making purposes.

2.2. Construction of the numerical reservoir model and determining process variables

The reservoir model constructed for flow-simulation in a tight-gas sand reservoir is a 2-dimensional (1-layer) system with a rectangular pattern with non-uniform grid distribution. The reservoir is fully saturated with gas due to the fact that water-phase is typically immobile in tight-gas reservoirs (Crotti, 2007; Moore et al., 2016). There is a horizontal-well at the center of the pattern producing under the constraint of constant flowing bottom-hole pressure (p_{wf}). Duration of the production is set as a 10-year period to consider a realistic tight-gas production scenario. Hydraulic fractures propagate in the direction of the maximum principal stress and perpendicular to the minimum principal stress. Since most hydraulically fractured wells are deeper than 1500 ft, hydraulic fractures are usually in vertical and transverse form (Soliman et al., 2008). Fig. 3 shows the top-view of the model for reservoirs with hydraulic fractures. Britt and Smith (2009) investigated and modeled a real tight-gas case study by using similar single-well simulation technique. In their study, it is noted that the anticipated fracture length (L_f) is 2000 feet, where the optimum number of completions/fractures (n) varies between 7 and 11. Also, Medeiros et al. (2008) studied productivity and drainage area of fractured horizontal wells in tight-gas reservoirs with a similar single-well simulation technique. In their study, discrete fractures have 200 ft of half-length (x_f) and 1000 md of fracture permeability (k_f),
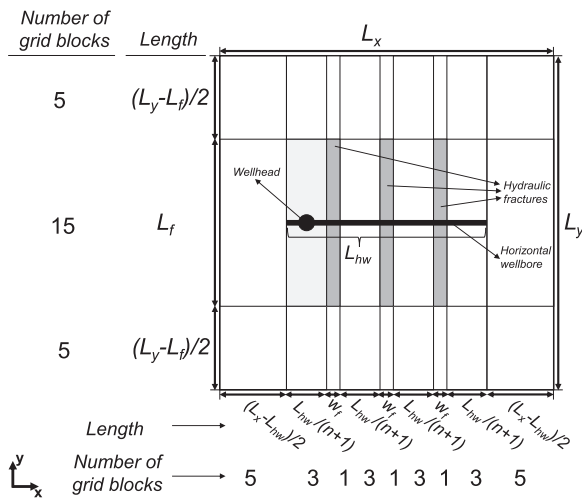
Fig. 3. Top view of the numerical reservoir model with transverse hydraulic fractures (there are 3 hydraulic fractures in this case).

Table 1

Ranges of input parameters used in generating training data using the numerical reservoir model, where outputs are the coefficients for production performance, *a*, *b*, and *c*.

Parameter	Minimum value	Maximum value	Unit
Initial conditions of the reservoir			
Area ($A = L_x \times L_y$)	40	2000	acres
Reservoir temperature (T)	80	280	F°
Initial reservoir pressure (p_i)	1000	8000	psi
Specific gravity of gas (γ_g)	0.6	0.9	
Reservoir characteristics			
(Uncontrollable parameters related to reservoir and hydraulic fracture effectiveness)			
Thickness (h)	50	400	ft
Permeability (k)	0.000001	0.1	md
Porosity (ϕ)	3	25	%
Fracture length ($L_f = 2x_f$)	400	2000	ft
Fracture permeability (k_f)	1000	100,000	md
Fracture width (w_f)	0.1	0.4	inches
Operational parameters			
(Controllable parameters related to horizontal well and hydraulic fracture design)			
Flowing bottom-hole pressure (p_{wf})	14.7	$0.5p_i + 14.7$	psi
Number of fractures (n)	1	30	
Horizontal wellbore length (L_{hw})	1000	8000	ft

which represent the minimum values of these parameters in our simulations considering the technological developments in this area. Holditch et al. (1993) estimated hydraulic fracture height (h_f) and width (w_f) by using radioactive tracer technology in various tight gas sand formations. Their study shows that fracture height, h_f, values vary from 50 to 400 ft and fracture width, w_f, values vary from 0.1 to 0.4 in.

Horizontal wellbore technology has improved rapidly in the last decade with lateral lengths that can reach up to 9500 ft in tight-gas sandstone reservoirs, such as the wells in the Granite Wash tight-gas reservoir in Texas and south-west Oklahoma (Wei and Xu, 2016). Longer horizontal wellbores directly impact the drainage area of the models that are used, where the range varies from 40 acres to 2000 acres. Significant increments in horizontal wellbore lengths have also created more room for the number of hydraulic fracture treatments. Therefore, a considerably large range of number of fractures is included in the model to develop a tool that can cover technological advancements in hydraulic fracturing operations, which changes from

1 to 30 discrete fractures. The model is designed in a way that the number of grid blocks change as the number of fractures change and hydraulic fractures are regularly spaced. The model has a fixed number of 25 grid blocks in the y-direction (N_y) and the number of gridblocks in the x-direction (N_x) is defined as, $13 + 4n$, as a function of the number of fractures (n). Therefore, as an example, if there are 3 hydraulic fractures in a given case, then the model has 25×25 grid blocks (see Fig. 3). However, if there are 30 fractures, it has 133×25 grid blocks. This configuration allows to have sufficient number of grid blocks between the hydraulic fractures and between the wellbore and drainage-area boundaries such that the fluid-flow dynamics are captured.

Although there are common physical and chemical processes controlling tight-gas sand properties, every single tight-gas reservoir is unique in terms of reservoir properties. Therefore, to acquire a utilizable and functional tool for hydraulically-fractured horizontal wells in tight gas reservoirs, a wide range of rock and fluid properties is determined. Table 1 shows the ranges of all parameters that are selected together with their ranges.

2.3. Construction of the knowledge base using performance indicators

To be able to construct a knowledge base that includes the corresponding performance indicators for each set of process input variables, the performance indicator must be clearly defined. The main performance indicator for any hydrocarbon reservoir is the cumulative recovery, which is a function of how the production rate declines with time. The time-dependent decline behavior of the production rate, namely the decline curve, can be mathematically characterized with certain coefficients. After carefully investigating the possible use of various decline curves such as the 2nd order exponential decline curve, the power law loss-ratio rate decline curve (Ilk et al., 2008), logarithmic decline curve with 4 parameters; Arps' hyperbolic decline curve (Arps, 1945) is selected to represent the production profiles used in this study:

$$q = \frac{q_i}{(1 + mD_i t)^{\frac{1}{m}}} \text{ or } q = \frac{a}{(1 + bt)^c} \tag{1}$$

Arps' hyperbolic decline curve provides consistent and good results for a wide variety of tight gas reservoir conditions (Table 1), which was also demonstrated with earlier real-case and numerical studies (Holditch, 2006; Rushing et al., 2007b, 2007a; Ilk et al., 2008). For all cases, hyperbolic decline curve was fit with a correlation coefficient of almost 1.00. On the basis of Eq. (1), the flow rate q, is a function of time t, and a is equal to q_i, which is the initial flow rate (Arps, 1945). In Eqn. (1), empirical coefficient b is considered as the product mD_i, which is the initial decline rate (D_i) coefficient multiplied by the hyperbolic-decline coefficient, m (Arps, 1945). Coefficient c is equal to $1/m$. Note that the empirical coefficient c is a function of coefficient b, and they vary in each production profile (Arps, 1945). Among the cases studied, the b coefficient was found to be in the range 5E-05 to 0.08 1/year, and c coefficient was found to be in the range 0.5–4.0. Based on this decline curve definition, coefficients a, b, and c were decided upon to be used as the performance characteristics for the tight-gas model. Using these coefficients rather than actual rates at certain times provides the flexibility of obtaining the performance characteristics at any desired time scale.

2.4. Construction of the neural-network based data-driven model

The purpose of data-driven modeling in this study is to develop a tool that can provide an estimation of the horizontal-well performance in a given tight-gas sand reservoir. Table 1 shows input variables that are used in the development of the model. It was desired to have 13 inputs that includes drainage area (A), reservoir thickness (h), permeability (k), porosity (ϕ), temperature (T), initial pressure (p_i), length of
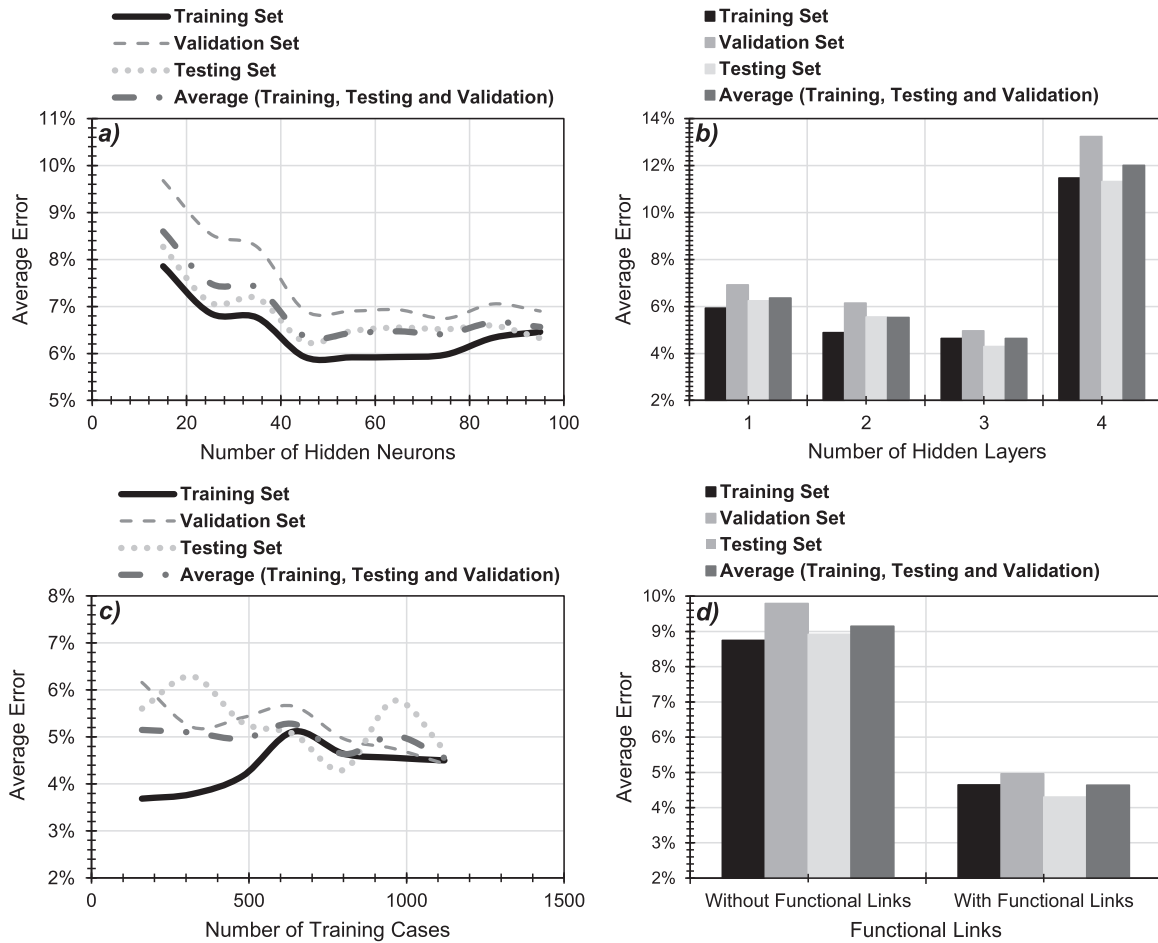
Fig. 4. Results of the manual optimization study for neural network design parameters for the data-driven model: a) Number of hidden neurons, b) Number of hidden layers, c) Number of training cases, d) Functional links.
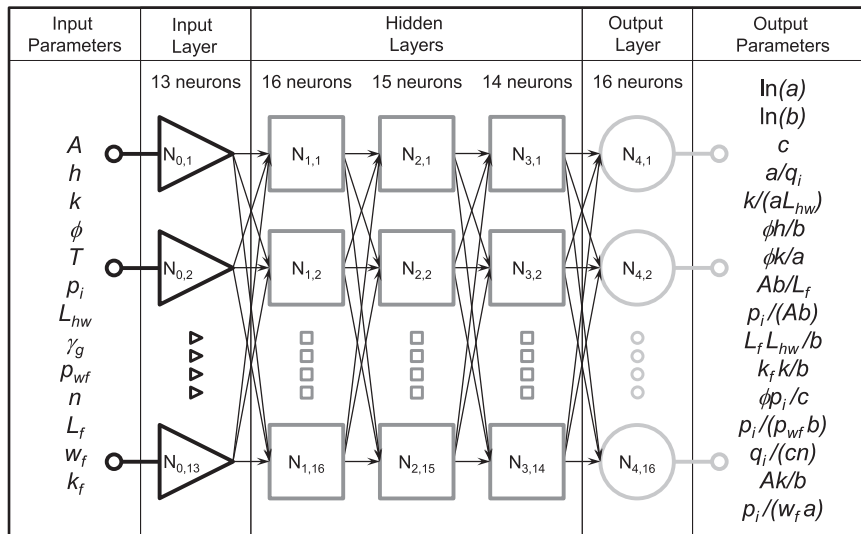

Fig. 5. The neural-network topology of the data-driven model with 13 input and 16 output parameters, and 16, 15, and 14 neurons in each hidden layer, respectively.

the horizontal well (L_{hw}), gas gravity (γ_g) and flowing bottom-hole pressure (p_{wf}). The model design also includes parameters related to hydraulic-fracture design and effectiveness. These parameters are the number of fractures (n), the length of hydraulic fractures (L_f), the width of hydraulic fractures (w_f), and the fracture permeability (k_f). Main output variables are the hyperbolic decline-curve coefficients: a, b, and c. Uniformly-distributed data sets within the minimum and

maximum values listed in Table 1 for each variable were generated. It was determined to divide the data set as the following:

- 80% for training,
- 10% for validation during training,
- 10% for testing the cases that were not presented to the neural network during training (blind-testing cases).

	k, md	*φ*
Minimum	0.05	0.08
Most Likely	0.07	0.11
Maximum	0.1	0.14
Distribution	Triangular	Normal

1. Assign probability distributions and ranges of uncertain input parameters.

n	*k, md*	*φ*
1	0.05	0.095
2	0.075	0.013
3	0.04	0.081
4	0.06	0.089
⋮	⋮	⋮
10,000	0.042	0.0125

2. Generate a dataset of each uncertain parameter using a random number generation algorithm such that it has the same probability distribution assigned in Step 1. Each set of parameters represents a case to run.

$$k_n \quad \varphi_n \rightarrow \text{[neural network]} \rightarrow G_{pn} \qquad n = 1, 2, 3, \ldots, 10{,}000$$
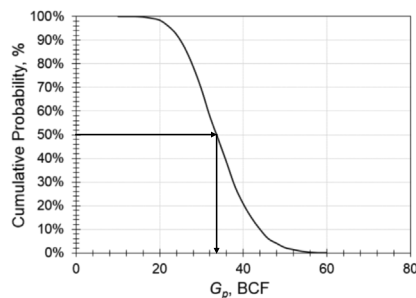
4. Analyze the cumulative probability distribution of the predicted output parameters and report the values that correspond to probabilities of interest.
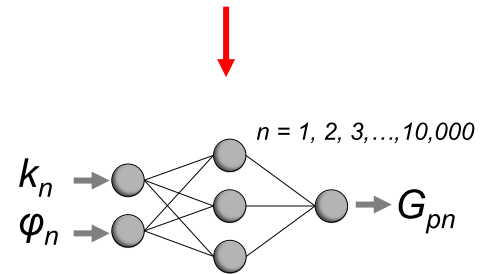
3. Predict the output parameters for each set of uncertain parameters using the data-driven forecasting tool.

Fig. 6. The workflow followed for probabilistic assessment of tight-gas sand reservoirs that utilizes the data-driven model to perform Monte Carlo simulation.

Table 2
Ranges and values of parameters used in the case study for probabilistic assessment.

Initial conditions of the reservoir (constant)

Parameter	Value
Area ($A = L_x \times L_y$)	372 acres
Reservoir temperature (T)	140°F
Initial reservoir pressure (p_i)	4000 psi
Specific gravity of gas (γ_g)	0.8

Reservoir characteristics

(Uncontrollable parameters related to reservoir and hydraulic fracture effectiveness)

Parameter	Minimum	Most-likely	Maximum
Thickness (h)	150 ft	200 ft	250 ft
Permeability (k)	0.01 md	0.02 md	0.03 md
Porosity (ϕ)	0.05	0.10	0.15
Fracture length ($L_f = 2x_f$)	800 ft	900 ft	1000 ft
Fracture permeability (k_f)	6000 md	8000 md	10,000 md
Fracture width (w_f)	0.16 in.	0.20 in.	0.24 in.

Operational parameters

(Controllable parameters related to horizontal well and hydraulic fracture design)

Parameter	Value
Flowing bottom-hole pressure (p_{wf})	1000 psi
Number of fractures (n)	10, 20, or 30 (depending on the scenario)
Horizontal wellbore length (L_{hw})	2,000, 4000 or 6000 ft (depending on the scenario)

Table 3
Summary of statistics of absolute errors of the output variables in the data-driven model for the training set (800 cases), validation set (100 cases), testing set (100 cases) and all cases (1000 cases).

|		a (%)	b (%)	c (%)	10-year Recovery (%)
Training Set	Mean	3.1	6.9	4.6	3.2
	Median	2.6	4.3	3.7	2.6
	Standard Deviation	2.6	9.8	4.0	2.7
	Minimum	0.004	0.012	0.00003	0.003
	Maximum	18.8	110.9	33.6	20.7
Validation Set	Mean	3.1	8.2	5.3	3.3
	Median	2.1	5.9	4.2	2.8
	Standard Deviation	2.9	8.1	4.7	2.7
	Minimum	0.162	0.004	0.11	0.075
	Maximum	14.5	53.6	23.8	12.7
Testing Set	Mean	3.1	6.9	4.6	3.2
	Median	2.3	3.9	3.5	2.5
	Standard Deviation	3.1	9.5	3.9	2.5
	Minimum	0.33	0.001	0.001	0.02
	Maximum	22.0	57.7	16.3	13.3
All	Mean	3.1	7.0	4.7	3.2
	Median	2.6	4.5	3.7	2.6
	Standard Deviation	2.7	9.6	4.0	2.7
	Minimum	0.004	0.001	0.00003	0.003
	Maximum	22.0	110.9	33.6	20.7
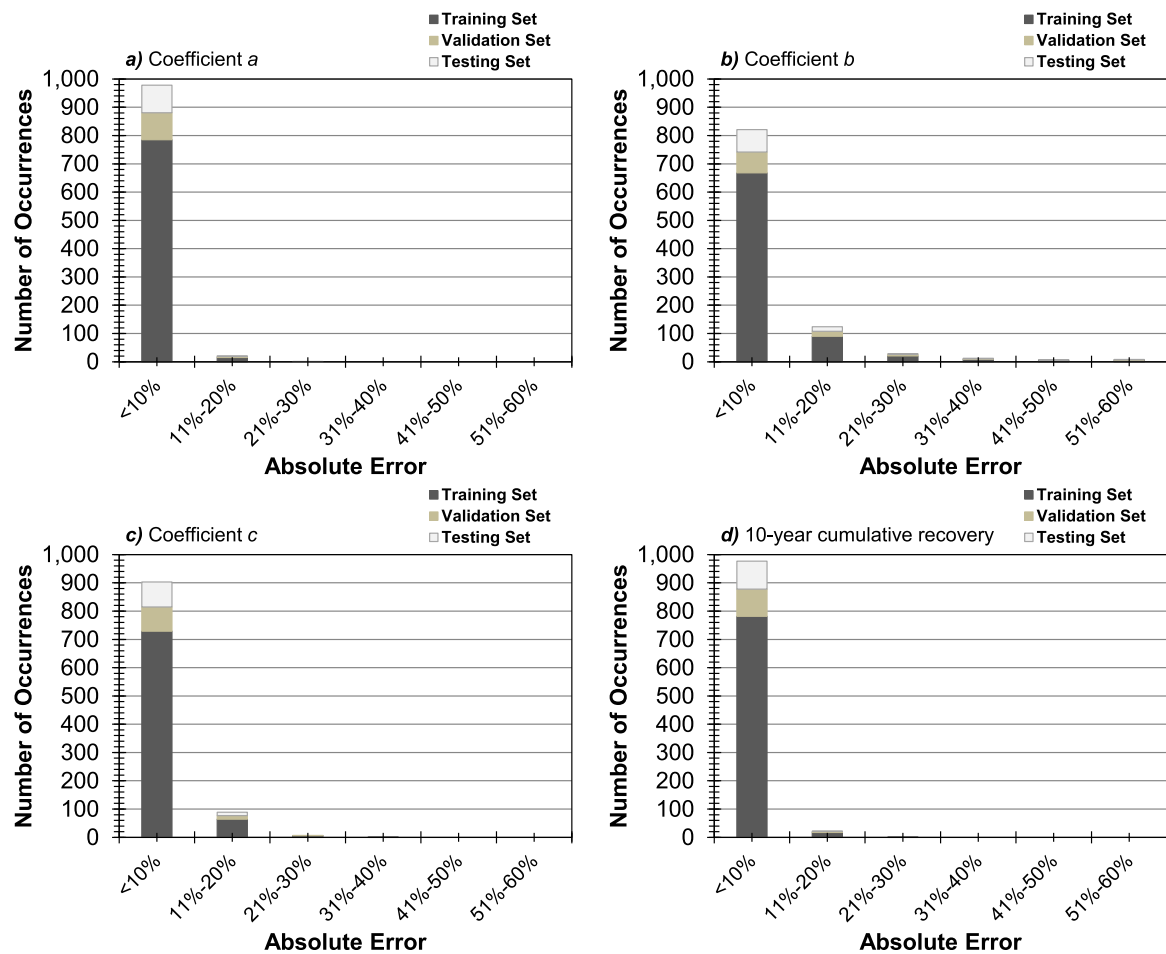
Fig. 7. Error frequencies of output parameters predicted by the data-driven model observed in the training, validation and testing sets: a) Coefficient *a*, b) Coefficient *b*, c) Coefficient *c*, d) 10-year cumulative recovery.

After acquiring these data sets for the numerical reservoir model and running them, corresponding performance indicators are collected. MATLAB Neural Network Toolbox (MATLAB, 2013) is used to train the network by using the data in the knowledge base. After testing a number of possible combinations of hidden-neuron numbers, the final design had three hidden layers and the layers had 16, 15, 14 neurons, respectively. This topology was determined after a manual-optimization study that required changing the numbers of hidden layers and hidden neurons. As shown in Fig. 4-a, optimum number of hidden neurons was determined as 45. Then, it was tested to try allocating 45 hidden neurons to different numbers of layers. As shown in Fig. 4-b, lowest average error was obtained with three layers with each having 16-15-14 neurons, respectively. The next step was to optimize the number of training cases to include. Fig. 4-c shows the average error changing with respect to the number of training cases. Although varying errors for different sets were observed with different numbers of cases, we decided to include 800 training cases, 100 validation and 100 testing cases, after considering the low error ranges for validation and testing sets. It was observed that representing hyperbolic coefficients *a* and *b* with their natural logarithm improved the training performance. The transfer function of the hidden layer neurons was set as the hyperbolic tangent sigmoid function while the output layer's transfer function was chosen to be linear, as also suggested in other studies (Hornik et al., 1989). Hyperbolic tangent sigmoid function activation function is differentiable and commonly used in multilayer networks that are trained using backpropagation algorithms (Demuth and Beale, 2002). A cascade-forward network which includes a weight connection from the input parameters to each layer and from each layer to the successive layers, is utilized, with scaled conjugate-gradient

backpropagation algorithm (Hagan et al., 2014). Gradient descent with momentum weight and bias learning function is used and mean squared error with regularization performance function is selected to evaluate the training performance (Hagan et al., 2014). The final step in the optimization process was to determine the contribution of functional links, which provide relationships between input and output parameters and help to achieve better training performance. These functional links are included in the output layer of the network in a way that they make additional information available to the output variables by introducing simple interactions of the Darcy's Law and original-gas-in-place equation parameters in regards to the fluid dynamics and storage in the reservoir, respectively, which have direct impact on the well performance. Benefits of including functional links were also demonstrated in similar studies (Guler et al., 2003; Ramgulam et al., 2007; Artun et al., 2012; Parada and Ertekin, 2012). As shown in Fig. 4-d, functional links helped to improve the average error from 9.2% to 4.6%. The final topology of the neural network is shown in Fig. 5 and there were 13 functional links added to the three hyperbolic decline curve coefficients as output parameters.

2.5. Probabilistic assessment using the data-driven model

The most important benefit of data-driven model can be demonstrated, when a significantly large number of simulations (i.e., in the range of thousands) are required while not having sufficient time, manpower and computational resources to perform so many simulations. A typical example for this situation is when some parameters can better be defined with a probability distribution, rather than certain values. This is, in fact, typically the case in problems related to
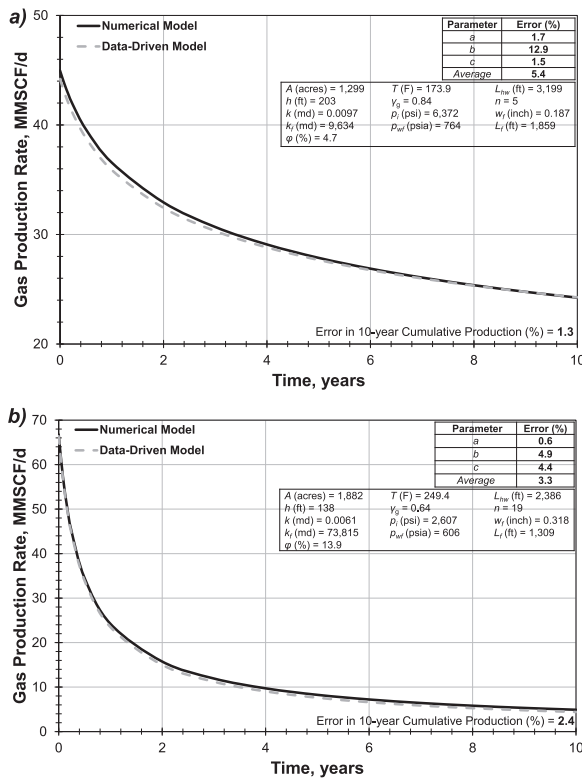
Fig. 8. Two of the relatively better forecasted production profiles: a) Average coefficient estimation error=5.4%, b) Average coefficient estimation error=3.3%.
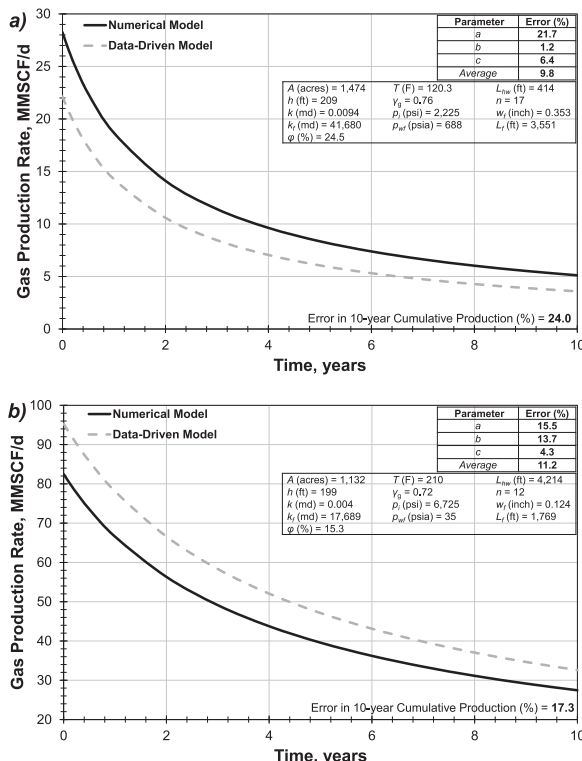

Fig. 9. Two of the relatively worse forecasted production profiles: a) Average coefficient-estimation error=9.8%, b) Average coefficient-estimation error=11.2%.

subsurface resources where hard data are available only from wellbores at isolated locations throughout the reservoir. In such kind of problems, it is better to define distribution functions and ranges of input parameters. Monte Carlo simulation can be performed by

generating a large number of scenarios that fit into pre-defined distribution functions. These scenarios can be generated by using random number generation algorithms that utilizes the characteristics of the distribution function. Once all the scenarios are simulated, probability distribution of output parameters can be analyzed and the uncertainty range can be quantified. This workflow is summarized in Fig. 6.

To demonstrate the practical application of the developed data-driven model, a case study is designed to perform a probabilistic assessment by considering the characteristics of the Williams Fork Formation. A horizontal well with multiple hydraulic fractures is taken into consideration. It is assumed to have uncertainty related to reservoir characteristics (porosity, thickness, and permeability) and hydraulic-fracture parameters (length, width and permeability of hydraulic fractures). The parameters are statistically defined with a triangular distribution with pre-defined minimum, maximum and most-likely values which are taken from published papers in the literature for the Williams Fork Formation (Ely et al., 1995; Reeves et al., 1999a, 1999b). A Monte Carlo simulation is performed by varying these parameters 10,000 times together with a given set of initial conditions and controllable operational parameters. Three scenarios are considered to analyze the sensitivity of the horizontal-well performance to the horizontal-well length and number of hydraulic fractures:

1. 2000-ft well with 10 hydraulic fractures,
2. 4000-ft well with 20 hydraulic fractures,
3. 6000-ft well with 30 hydraulic fractures.

The values and ranges of all parameters are shown in Table 2. Using the data-driven model, the expectation curves for cumulative gas recoveries are obtained and compared with the results obtained with same number of cases using the numerical-model.

3. Results and discussion

3.1. Estimation of horizontal-well performance

The main goal of the data-driven forecasting tool is to predict the performance of the well in the form of the decline-curve coefficients a, b, and c. It should be noted that the proposed model predicts the natural logarithm of coefficients a and b (Fig. 5). Therefore, $\ln(a)$ and $\ln(b)$ values are needed to be converted to their original values to calculate actual error values. Otherwise, very small, unrealistic and misleading percent errors are encountered because of the compression of errors in the logarithmic scale. The other error analysis method is the assessment of the accuracy of cumulative production. By using coefficients, a, b and c obtained from the numerical model, and the values predicted by the data-driven model (a_{DDM}, b_{DDM} and c_{DDM}); the error associated with the cumulative gas production at a given time, t, is calculated for each case:

$$Error_{cum}(\%) = \frac{\left| \int_0^t \frac{a}{(1+bt)^c}dt - \left(\int_0^t \frac{a}{(1+bt)^c}dt \right)_{DDM} \right|}{\int_0^t \frac{a}{(1+bt)^c}dt} \times 100 \qquad (2)$$

The average error of the cumulative-production prediction highlights the combined effects of the coefficients all together. Table 3 shows the summarized statistics of errors for coefficients a, b and c, together with the cumulative recovery after 10 years for training, validation, testing cases and all sets together. The testing set is the most critical data set for validation purposes, since it is the set that was not presented to the model during the training process. If we analyze the error levels for this set, we observe that the coefficient a has an average absolute error of 3.1%. When compared with other coefficients, b and c,
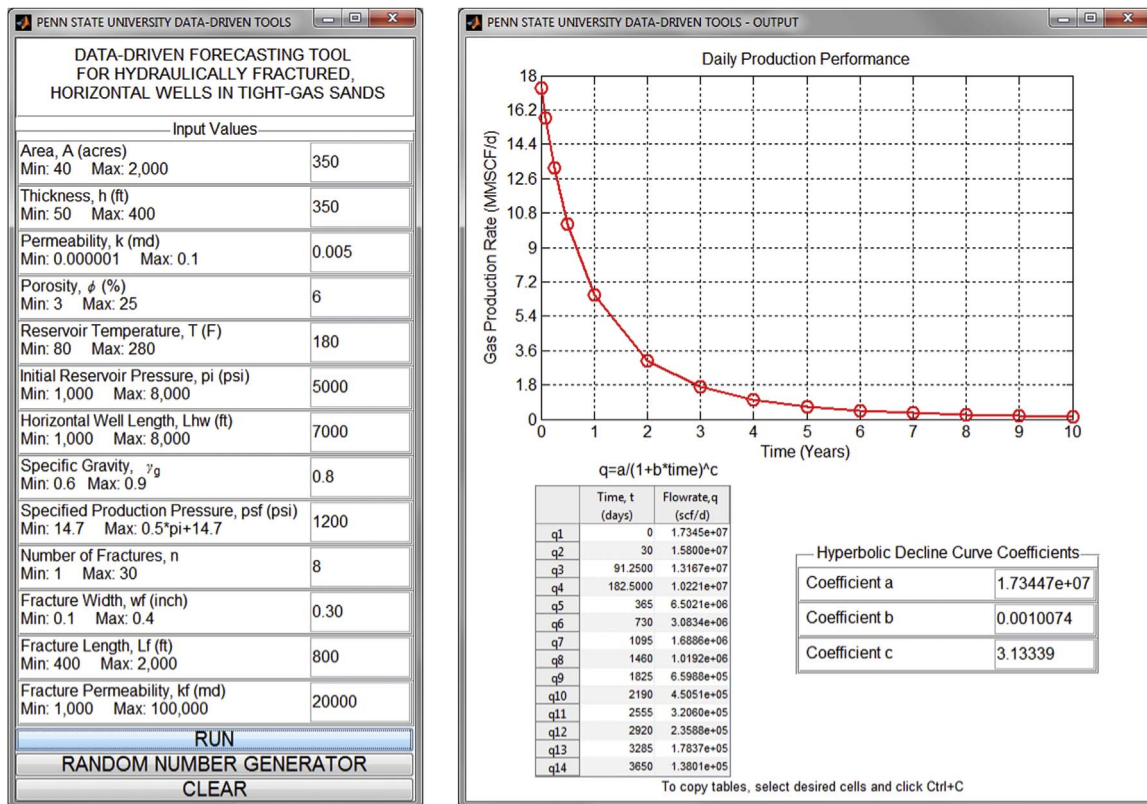
Fig. 10. Graphical-user-interface application (GUI) for the forecasting tool that allows to interactively input the required parameters (left) and visualize the output of the model (right).

it is observed that *a* is the coefficient that was predicted with the highest accuracy. It is the numerator of the hyperbolic decline curve and it should be predicted as close as possible to the initial gas-production rate of each case. Therefore, it has the largest impact on the quality of the developed model. Although coefficient *b* has a greater error (6.9%) than the other coefficients, it has a relatively smaller impact on the trend of the hyperbolic decline-curve profile. Therefore, it is rather acceptable for the coefficient *b* to have greater error values than other coefficients in determining the quality of the prediction. It is observed that the prediction of the coefficient *c* has a significant effect on the hyperbolic decline-curve profile. Coefficient *c* values are found to be within a range between 0.5 and 4.0 which is relatively narrower than the range of variation of coefficient *b*. This eventually helped the model to achieve a better prediction accuracy for the coefficient *c* with an average absolute error of 4.6%. Average error of all three coefficients is 4.9%.

Analysis of the cumulative gas production error provides insights about the overall impact of the coefficients, since the cumulative production is the area under the declining curve of the daily production rate. The average error for the cumulative production is 3.2%, which shows that the recovery can be predicted within reasonable accuracy levels, as compared with the numerical model. The error is calculated for cumulative production of 10 years for illustration purposes, considering a typical production period for a tight-gas sand well. It should be noted that cumulative production errors for different time periods may slightly vary. Fig. 7 shows the frequency distributions of errors of output parameters predicted by the model as observed in the training, validation and testing sets. These error frequencies indicate that the majority of the cases experienced an error that is less than 10% in training, validation and testing sets. This also gives confidence about the prediction capabilities of the model.

Fig. 8 shows production rate vs. time profiles of two of the better cases, in terms of prediction accuracy. The cumulative production error is 1.3% in Fig. 8-a and 2.4% in Fig. 8-b. Note that the errors of

coefficient *b* values are rather high in these figures (12.9% and 4.9%). These errors show that the prediction performance of coefficient *b* has a rather low impact on the overall prediction performance of the model, when compared with other coefficients. Figs. 9-a and 9-b show two of the relatively worse cases. These two figures confirm that the prediction of coefficient *a* is substantially important. In Figs. 9-a and 9-b, although the percent errors of coefficients *b* and *c* vary, predicted production performances follow similar patterns, which shows that the impact of the errors of coefficient *b* and *c* are lower on the overall quality of the prediction. Production profiles appear to be slightly over- and under-estimated, respectively, because coefficient *a* values could not be predicted as desired by the model in these two cases. This also directly affects the cumulative-recovery errors negatively.

To convert the model into a user-friendly tool for the practicing engineer, a graphical-user-interface (GUI) application is developed that uses the model to provide estimated quantities of the outputs once the required input parameters are provided (Fig. 10). The simulation models of complex tight-gas sand reservoirs and their advanced wellbore designs with hydraulic fractures can cause excessive simulation times if not trigger convergence problems or simulation failures. Data-driven modeling is one of the supplementary tools to overcome aforementioned problems. The forecasting tool developed in this study not only helps to reduce simulation time requirements or related simulation failures, but also enhances the overall decision-making process by using it as a faster proxy to conventional numerical simulators when needed. Each simulation run completed with the numerical model used in this study takes around 5 min depending on the complexity of the case on an Intel ® Core™ i7-M640 2.80 GHz CPU. Considering the software requirements and the time that is required for pre-processing, building, validation and post-processing all together, the full cycle of modeling would require significant amount of time and monetary investments. On the other hand, the data-driven model can output the estimates of performance characteristics within a fraction of a second, providing engineers with significant savings in
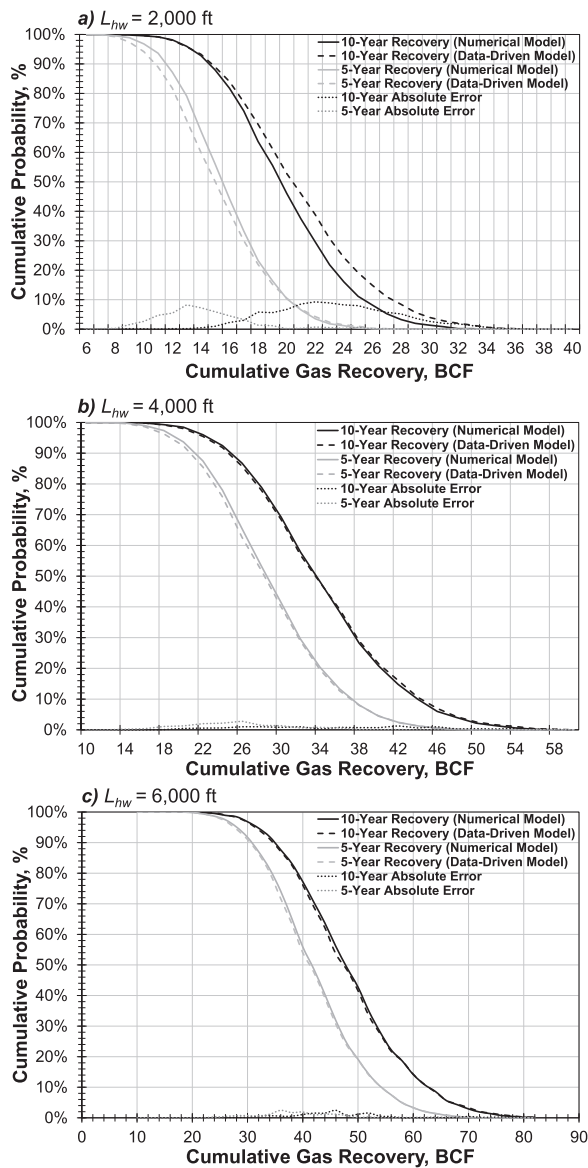
Fig. 11. Expectation curves of cumulative recovery after 5 and 10 years of production obtained from the numerical-model and data-driven model for different well designs: a) 2000 ft with 10 fractures, b) 4000 ft with 20 fractures, c) 6000 ft with 30 fractures.

terms of expended resources.

3.2. Case study: probabilistic assessment of tight-gas reservoirs

After performing a Monte Carlo simulation for 10,000 cases, cumulative recoveries after 5 and 10 years are calculated using decline-curve coefficients *a*, *b*, and *c*, that are predicted by the data-driven model. For the purpose of re-validating the data-driven model, recoveries from the numerical model are also collected for the same set of 10,000 cases. Frequencies of cumulative recoveries are used to construct the expectation curves shown in Fig. 11. All well-design scenarios that are investigated are shown, with cumulative recoveries after 5 years and 10 years of production. Satisfactory matches between data-driven model and numerical-model derived probability values are obtained with error differences of within ± 10%. This demonstrates the possibility of running as many as 10,000 cases using the data-driven model within a fraction of a second with similar accuracy as a numerical reservoir model which required about 30 days of CPU time to run 10,000 cases on an Intel ® Core™ i7-M640 2.80 GHz CPU. Results of these cases can be used to perform a Monte Carlo simulation

Table 4
P10, P50 and P90 estimations of cumulative recovery in billion cubic feet (BCF) after 5 and 10 years of production obtained from numerical and data-driven models for different well designs.

L_{hw}=2000 ft, n=10 fractures				
	5-year Recovery		10-year Recovery	
Probability	**Numerical**	**Data-Driven**	**Numerical**	**Data-Driven**
10%	20.1	20.1	25.4	27.4
50%	15.5	15.0	19.6	20.4
90%	11.6	10.8	14.6	14.8

L_{hw}=4000 ft, n=20 fractures				
	5-year Recovery		10-year Recovery	
Probability	**Numerical**	**Data-Driven**	**Numerical**	**Data-Driven**
10%	36.6	36.6	44.0	44.2
50%	28.3	28.1	32.8	32.8
90%	20.6	20.3	24.4	24.3

L_{hw}=6000 ft, n=30 fractures				
	5-year Recovery		10-year Recovery	
Probability	**Numerical**	**Data-Driven**	**Numerical**	**Data-Driven**
10%	46.7	46.5	55.7	59.7
50%	38.6	37.9	44.1	44.8
90%	31.3	33.5	33.3	32.7

study to account for the uncertainties in reservoir and hydraulic-fracture parameters to see their impact on the well performance.

Table 4 shows the P10, P50, and P90 estimations from the cumulative probability curves shown in Fig. 11. These values are the values that the cumulative recovery would be greater than with probabilities of 10%, 50%, and 90%. P10, P50, and P90 values are also visually shown in Fig. 12, in which the match between the data-driven and numerical-model derived results is clearly seen. Such kind of an analysis allows us to compare different well designs with different numbers of hydraulic fractures along the well path within the ranges of known uncertainties. Recovery values can be incorporated to an economic analysis together with the costs associated with the length of the horizontal well and number of fractures to make important decisions regarding the operation of a given tight-gas reservoir.

3.3. Limitations of the forecasting tool

The presented tool has a wide range of applicability for the purpose of predicting the performance of hydraulically-fractured horizontal wells in tight-gas sands. Following are potential limitations to take into consideration when this tool is used:

1. Since the model is trained using results from a numerical-model, its predictive capability is limited to the numerical model's accuracy. Therefore, the assumptions defined during the numerical-model building process are also carried into the data-driven model. However, it must be noted that the purpose of this tool is not to replace or improve the accuracy of high-fidelity numerical models, but rather to use it as a proxy model to perform an efficient modeling study, or to reduce ranges of uncertainties prior to more detailed numerical-modeling studies.
2. Since the cases used for training are within the ranges of parameters presented in Table 1, the model may not be able to provide accurate predictions outside this range. While it was aimed to cover a wide range of possibilities and to study somewhat extreme conditions as
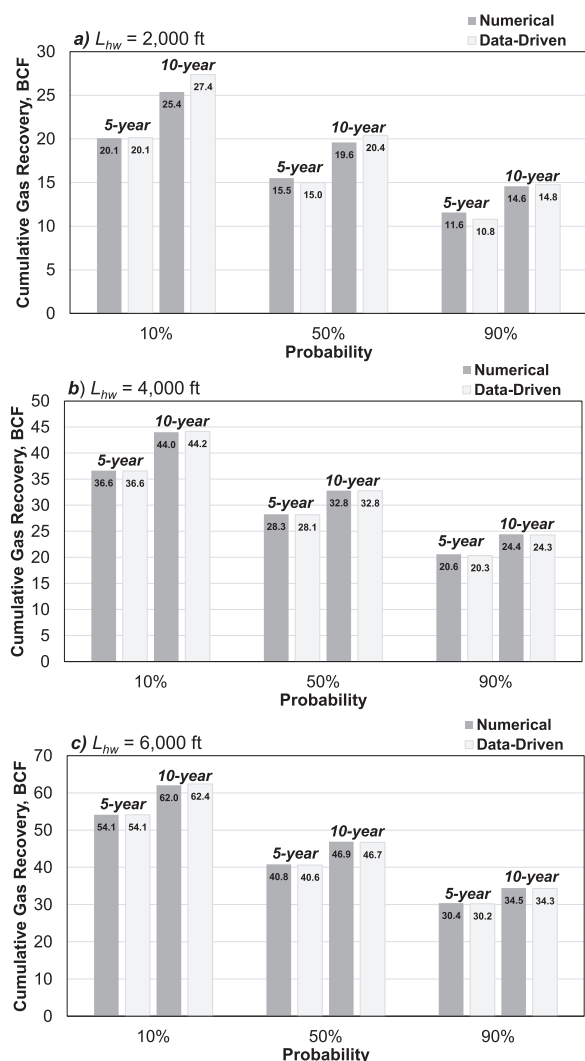
Fig. 12. Comparisons of P10, P50 and P90 estimations of cumulative recovery after 5 and 10 years of production obtained from the numerical-model and data-driven model for different well designs: a) 2000 ft with 10 fractures, b) 4000 ft with 20 fractures, c) 6000 ft with 30 fractures.

well, the dataset used should be expanded and the model should be re-trained for the purpose of inclusion of these new conditions. The methodology presented in this paper would provide the guidelines for such kind of a study.

3. Predicted well-performance is assumed to follow Arps' hyperbolic-decline curve as we were able to accurately fit this type of decline curve through the production behavior obtained from the numerical model. While the data-driven model can predict the performance within acceptable accuracy levels using a hyperbolic-decline curve, this curve may not be valid in some systems and under some conditions. In those situations, the prediction accuracy may suffer from the differences in the decline behavior.

4. Conclusions

In this study, a data-driven forecasting tool is developed and validated for tight-gas sands by combined utilization of artificial neural networks and a numerical reservoir model. The key conclusions are as follows:

1. The model is validated with blind cases in which the well performance coefficients are predicted with an average error of 4.9%, and the cumulative gas recovery after 10 years is predicted with an

average error of 3.2%.

2. The model can be used as a practical decision-making tool through the use of a graphical-user-interface application, which outputs the expected quantities of the related parameters within a fraction of second.

3. The model can be used to investigate many cases efficiently, as demonstrated with the case study for Williams Fork Formation through a probabilistic assessment of various well designs.

References

Abacioglu, Y., Sebastian, H., Oluwa, J., 2009. Advancing reservoir simulation capabilities for tight gas reservoirs. In: SPE Rocky Mountain Petroleum Technology Conference. No. SPE-122793-MS. 14-16 April, Denver, Colorado. http://dx.doi.org/10.2118/122793-MS.

Alizadeh, B., Najjari, S., Kadkhodaie-Ilkhch, A., 2012. Artificial neural network modelling and cluster analysis for organic facies and burial history estimation using well log data: a case study of the south pars gas field, persian gulf, iran. Comp. Geosci. 45, 261–269. http://dx.doi.org/10.1016/j.cageo.2011.11.024.

Amirian, E., Leung, J., Zanon, S., Dzurman, P., 2013. Data-driven modeling approach for recovery performance prediction in SAGD operations. In: SPE Heavy Oil Conference Proceedings. No. SPE-165557-MS. 11-13 June. Calgary, Alberta. http://dx.doi.org/10.2118/165557-MS.

Arps, J., 1945. Analysis of decline curves. Trans. AIME 160 (1), 228–247.

Artun, E., Mohaghegh, S., 2011. Intelligent seismic inversion workflow for high-resolution reservoir characterization. Comp. Geosci. 37 (2), 143–157. http://dx.doi.org/10.1016/j.cageo.2010.05.007.

Artun, E., Ertekin, T., Watson, R., Miller, B., 2010. Development and testing of proxy models for screening cyclic pressure pulsing process in a depleted, naturally fractured reservoir. J. Pet. Sci. Eng. 73 (1), 73–85. http://dx.doi.org/10.1016/j.petrol.2010.05.009.

Artun, E., Ertekin, T., Watson, R., Al-Wadhahi, M., 2011. Development of universal proxy models for screening and optimization of cyclic pressure pulsing in naturally fractured reservoirs. J. N. Gas Sci. Eng. 3 (6), 667–686. http://dx.doi.org/10.1016/j.jngse.2011.07.016.

Artun, E., Ertekin, T., Watson, R., Miller, B., 2012. Designing cyclic pressure pulsing in naturally fractured reservoirs using an inverse-looking recurrent neural network. Comp. Geosci. 38 (1), 68–79. http://dx.doi.org/10.1016/j.cageo.2011.05.006.

Artun, E., 2016. Characterizing interwell connectivity in waterflooded reservoirs using data-driven and reduced-physics models: a comparative study. Neural Comput & Applic. http://dx.doi.org/10.1007/s00521-015-2152-0.

Ayala, L., Ertekin, T., 2005. Analysis of gas-cycling performance in gas/condensate reservoirs using neuro-simulation. In: SPE Annual Technical Conference and Exhibition Proceedings. No. SPE-95655-MS. 9-12 October. Dallas, Texas. http://dx.doi.org/10.2118/95655-MS.

Baihly, J., Grant, D., Fan, L., Bodwadkar, S., 2009. Horizontal wells in tight gas sands - a method for risk management to maximize success. SPE Prod. Oper. 24 (02), 277–292. http://dx.doi.org/10.2118/110067-PA.

Britt, L., Smith, M., 2009. Horizontal well completion, stimulation optimization, and risk mitigation. In: SPE Eastern Regional Meeting Proceedings. No. SPE-125526-MS. 23-25 September, Charleston, West Virginia. http://dx.doi.org/10.2118/125526-MS.

Centilmen, A., Ertekin, T., Grader, A.S., 1999. Applications of neural networks in multiwell field development. In: SPE Annual Technical Conference and Exhibition Proceedings. No. SPE-56433-MS. 3-6 October. Houston, Texas. http://dx.doi.org/10.2118/56433-MS.

CMG, 2015. CMG IMEX Reservoir Simulation Software, version 2015. Computer Modeling Group, Ltd. Calgary, Alberta.

Crotti, M., 2007. Water saturation in tight gas sand reservoirs. In: SPE Latin American and Caribbean Petroleum Engineering Conference Proceedings. No. SPE-107145-MS. 1518 April, Buenos Aires, Argentina. http://dx.doi.org/10.2118/107145-MS.

Cullick, A., Johnson, D., Shi, G., 2006. Improved and more rapid history matching with a nonlinear proxy and global optimization. In: SPE Annual Technical Conference and Exhibition Proceedings. No. SPE-101933-MS. 24-27 September. San Antonio, Texas. http://dx.doi.org/10.2118/101933-MS.

Demiryurek, U., Banaei-Kashani, F., Shahabi, C., Wilkinson, F., 2008. Neural-network based sensitivity analysis for injector-producer relationship identification. In: SPE Intelligent Energy Conference and Exhibition Proceedings. No. SPE-112124-MS. 25-27 February. Amsterdam, The Netherlands. http://dx.doi.org/10.2118/112124-MS.

Demuth, H., Beale, M., 2002. Neural Network Toolbox for Use with MATLAB. Mathworks, Inc.,

Dong, Z., Holditch, S., McVay, D., Ayers, W., 2012. Global unconventional gas resource assessment. SPE Econ. Man 4 (4), 222–234. http://dx.doi.org/10.2118/148365-PA.

Doraisamy, H., Ertekin, T., Grader, A., 2000. Field development studies by neuro-simulation: an effective coupling of soft and hard computing protocols. Comp. Geosci. 26 (8), 963–973. http://dx.doi.org/10.1016/S0098-3004(00)00032-7.

Ely, J., Brown, T., Reed, S., 1995. Optimization of hydraulic fracture treatment in the Williams Fork Formation of the Mesaverde Group. In: SPE Rocky Mountain Regional/Low-Permeability Reservoirs Symposium Proceedings. No. SPE-29551-MS. 20-22 March. Denver, Colorado. http://dx.doi.org/10.2118/29551-MS.

Esmaili, S., Mohaghegh, S., 2016. Full field reservoir modeling of shale assets using advanced data-driven analytics. Geosci. Front. 7 (1), 11–20. http://dx.doi.org/10.1016/j.gsf.2014.12.006.

Gokcesu, U., Ertekin, T., Flemings, P., 2005. Application of neural networks and genetic algorithms in field development studies. In: 2nd Kuwait International Petroleum Conference and Exhibition Proceedings. 10-12 December. Kuwait City, Kuwait.

Guler, B., Ertekin, T., Grader, A., 2003. An artificial neural network based relative permeability predictor. J. Can. Pet. Technol. 42, 49–57. http://dx.doi.org/10.2118/03-04-02, (PETSOC-03-04-02).

Hagan, M., Demuth, H., Beale, M., de Jess, O., 2014. Neural Network Design 2nd edition. Martin Hagan.

Holditch, S., 2006. Tight gas sands. J. Pet. Technol. 58 (6), 86–93. http://dx.doi.org/10.2118/103356-JPT.

Holditch, S., Holcomb, D., Rahim, Z., 1993. Using tracers to evaluate propped fracture width. In: SPE Eastern Regional Meeting Proceedings. No. SPE-26922-MS. 2-4 November, Pittsburgh, Pennsylvania. http://dx.doi.org/10.2118/26922-MS.

Hornik, K., Stinchcombe, M., White, H., 1989. Multilayer feedforward networks are universal approximators. Neural Net. 2 (5), 359–366.

Ilk, D., Rushing, J., Perego, A., Blasingame, T., 2008. Exponential vs. hyperbolic decline in tight gas sands: Understanding the origin and implications for reserve estimates using Arps' decline curves. In: SPE Annual Technical Conference and Exhibition Proceedings. No. SPE-116731-MS. 21-24 September, Denver, Colorado. http://dx.doi.org/10.2118/116731-MS.

Iwere, F., Moreno, J., Apaydin, O., 2006. Numerical simulation of thick, tight fluvial sands. SPE Res. Eval. Eng. 9 (4), 374–381. http://dx.doi.org/10.2118/90630-PA.

Johnson, V., Rogers, L., 2001. Applying soft computing methods to improve the computational tractability of a subsurface simulation-optimization problem. J. Pet. Sci. Eng. 29 (3–4), 153–175. http://dx.doi.org/10.1016/S0920-4105(01)00087-0.

Kalantari-Dhaghi, A., Mohaghegh, S., Esmaili, S., 2015. Data-driven proxy at hydraulic fracture cluster level: a technique for efficient CO_2-enhanced gas recovery and storage assessment in shale reservoir. J. Nat. Gas. Sci. Eng. 27 (2), 515–530. http://dx.doi.org/10.1016/j.jngse.2015.06.039.

Law, B., Curtis, J., 2002. Introduction to unconventional petroleum systems. AAPG Bull. 86 (11), 1851–1852.

MATLAB, 2013. MATLAB Neural Network Toolbox, version 2013a. Mathworks, Inc., Natick, Massachusetts.

Medeiros, F., Ozkan, E., Kazemi, H., 2008. Productivity and drainage area of fractured horizontal wells in tight gas reservoirs. SPE Res Eval. Eng. 11 (5), 902–911. http://dx.doi.org/10.2118/108110-PA.

Metz, M., Briceno, G., Fang, Q., Diaz, E., Grader, A., Dvorkin, J., 2009. Properties of tight gas sand from digital images. In: SEG Annual Meeting. No. SEG-2009–2135. 25-30 October. Houston, Texas.

Mohaghegh, S., 2011. Reservoir simulation and modeling based on pattern recognition. In: SPE Digital Energy Conference and Exhibition Proceedings. No. SPE-143179-MS. 19-21 April. The Woodlands, Texas. http://dx.doi.org/10.2118/143179-MS.

Mohaghegh, S., Al-Mehairi, Y., Gaskari, R., Maysami, M., Khazaeni, Y., Gashut, M., Al-Hammadi, A., Kumar, S., 2014. Data-driven reservoir management of a giant mature oilfield in the Middle East. In: SPE Annual Technical Conference and Exhibition Proceedings. No. SPE-170660-MS. 27-29 October. Amsterdam, The Netherlands. http://dx.doi.org/10.2118/170660-MS.

Mohaghegh, S., Modavi, A., Hafez, H., Haajizadeh, M., Kenawy, M., Guruswamy, S., 2006. Development of surrogate reservoir models (SRM) for fast-track analysis of complex reservoirs. In: SPE Intelligent Energy Conference and Exhibition Proceedings. No. SPE-99667-MS. 11-13 April. Amsterdam, The Netherlands. http://dx.doi.org/10.2118/99667-MS.

Moore, W., Ma, Y., Pirie, I., Zhang, Y., 2016. Unconventional Oil and Gas Resources Handbook. Elsevier, Ch. 15: Tight gas sandstone reservoirs, part 2: Petrophysical analysis and reservoir modeling, pp. 429–448.

Parada, C.H., Ertekin, T., 2012. A new screening tool for improved oil recovery methods using artificial neural networks. In: SPE Western Regional Meeting Proceedings. No. SPE-153321-MS. 19-23 March. Bakersfield, California. http://dx.doi.org/10.2118/153321-MS.

Patel, A., Davis, D., Guthrie, C., Tuk, D., Nguyen, T., Williams, J., 2005. Optimizing cyclic steam oil production with genetic algorithms. In: SPE Western Regional Meeting Proceedings. No. SPE-93906-MS. 30 March - 1 April. Irvine, California. http://dx.doi.org/10.2118/93906-MS.

Raeesi, M., Moradzadeh, A., Ardejani, F., Rahimi, M., 2012. Classification and identification of hydrocarbon reservoir lithofacies and their heterogeneity using seismic attributes, logs data and artificial neural networks. J. Pet. Sci. Eng. 82–83, 151–165. http://dx.doi.org/10.1016/j.petrol.2012.01.012.

Ramgulam, A., Ertekin, T., Flemings, P.B., 2007. An artificial neural network utility for the optimization of history matching process. In: SPE Latin American & Caribbean Petroleum Engineering Conference Proceedings. No. SPE-107468-MS. 15-18 April. Buenos Aires, Argentina. http://dx.doi.org/10.2118/107468-MS.

Reeves, S., Hill, D., Hopkins, C., Conway, M., Tiner, R., Mohaghegh, S., 1999a. Restimulation technology for tight gas sand wells. In: SPE Annual Technical Conference and Exhibition Proceedings. No. SPE-56482-MS. 3-6 October, Houston, Texas. http://dx.doi.org/10.2118/56482-MS.

Reeves, S., Hill, D., Tiner, R., Bastian, P., Conway, M., Mohaghegh, S., 1999b. Restimulation of tight gas sand wells in the rocky mountain region. In: SPE Rocky Mountain Regional Meeting Proceedings. No. SPE-55627-MS. 15-18 May, Gillette, Wyoming. http://dx.doi.org/10.2118/55627-MS.

Rushing, J., Newsham, K., Perego, A., Comisky, J., Blasingame, T., 2007a. Beyond decline curves: life-cycle reserves appraisal using an integrated work-flow process for tight gas sands. In: SPE Annual Technical Conference and Exhibition Proceedings. No. SPE-109836-MS. 11-14 November, Anaheim, California. http://dx.doi.org/10.2118/109836-MS.

Rushing, J., Perego, A., Sullivan, R., Blasingame, T., 2007b. Estimating reserves in tight gas sands at HP/HT reservoir conditions: use and misuse of an Arps decline curve methodology. In: SPE Annual Technical Conference and Exhibition Proceedings. No. SPE-109625-MS. 11-14 November, Anaheim, California. http://dx.doi.org/10.2118/109625-MS.

Silva, P., Maschio, C., Schiozer, D., 2007. Use of neuro-simulation techniques as proxies to reservoir simulator: application in production history matching. J. Pet. Sci. Eng. 57 (3–4), 273–280. http://dx.doi.org/10.1016/j.petrol.2006.10.012.

Smith, T., Sayers, C., Sondergeld, C., 2009. Rock properties in low-porosity/low-permeability sandstones. Lead. Edge 28, 24–59.

Soliman, M., East, L., Ansah, J., Wang, H., 2008. Testing and design of hydraulic fractures in tight gas formations. In: SPE Russian Oil & Gas Technical Conference and Exhibition Proceedings. No. SPE-114988-RU. 28-30 October, Moscow, Russia. http://dx.doi.org/10.2118/114988-RU.

Solomatine, D., See, L., Abrahart, R., 2008. Practical Hydroinformatics. Vol. 68. Springer, Ch. 2: Data-driven modeling: concepts, approaches and experiences, pp. 17–30.

Wei, Y., Xu, J., 2016. Unconventional Oil and Gas Resources Handbook. Elsevier, Ch. 16: Granite Wash tight gas reservoir, pp. 449–473.

Zangl, G., Giovannoli, M., Stundner, M., 2006. Application of artificial intelligence in gas storage management. In: SPE Europec/EAGE Annual Conference and Exhibition Proceedings. No. SPE-100133-MS. 12-15 June. Vienna, Austria. http://dx.doi.org/10.2118/100133-MS.